Acid Dissociation of HBr on a Model Ice Surface†

Ayman Al-Halabi,‡ Roberto Bianco,§ and James T. Hynes*,§,||

Leiden Institute of Chemistry, Gorlaeus Laboratories, Leiden University, Einsteinweg 55, P.O. Box 9502 2300 RA, Leiden, The Netherlands, Department of Chemistry and Biochemistry, University of Colorado, Boulder, Colorado 80309-0215, and Departement de Chimie, CNRS UMR 8640 PASTEUR, Ecole Normale Supérieure, 24 rue Lhomond, Paris 75231, France

Received: February 7, 2002; In Final Form: April 25, 2002

The acid ionization of HBr on ice is important in connection with the rapid springtime ozone depletion in the Arctic tropospheric boundary layer. The interaction of HBr with an ice surface is studied theoretically via electronic structure calculations on a semiconstrained $HBr\cdot(H_2O)_{13}$ model cluster at the MP2 level of theory using effective core potentials for all the heavy atoms. The heterolytic dissociation of HBr to form a $H_3O^+\cdot Br^-$ contact ion pair is not found to occur atop this model ice lattice system, but it is found to be barrierless and energetically spontaneous when assisted by a single extra-lattice water molecule.

1. Introduction

It is now well recognized that heterogeneous reactions occurring on aerosol surfaces, including ice aerosols, play a critical role in ozone depletion in the polar stratosphere and elsewhere.[1,2] For example, the net reaction $HCl + ClONO_2 \rightarrow Cl_2 + HNO_3$[1] between the so-called "reservoir species", i.e., inactive from the purely gas-phase point of view, hydrochloric acid HCl and chlorine nitrate $ClONO_2$ to produce photolyzable chlorine is recognized as the key heterogeneous reaction in the Antarctic stratosphere connected to extensive ozone depletion there.[1,2]

Considerable attention, both experimental and theoretical (for a partial listing, see refs 3−8) has consequently been given to the issue of the acid ionization of HCl at or on an ice surface, since this is central to the question of the ionic or molecular character of the cited $HCl + ClONO_2$ reaction and its variants. The corresponding question for hydrobromic acid HBr has received less attention,[9−15] particularly from a theoretical viewpoint.[16−18] In this paper, we present electronic structure calculations to examine the possibility of the HBr acid ionization, proton-transfer reaction

$$HBr + H_2O \rightarrow Br^- + H_3O^+ \qquad (1)$$

atop a cluster model $HBr\cdot(H_2O)_{13}$ of an ice surface. Although the molecular level explication of reaction 1 is clearly of interest in connection with the numerous experiments that address it,[9−15] it is also important to consider its relevance for ozone depletion in various atmospheric contexts. As now recounted, the significant atmospheric relevance of reaction 1 is likely to be confined to the Arctic tropospheric boundary layer.

In the polar (Antarctic and Arctic) stratosphere, heterogeneous bromine chemistry has been implicated in ozone depletion,[19] although this does not necessarily imply any significant role for HBr. Important features here are that, despite the lower concentration of bromine compared to chlorine compounds, bromine has a higher capacity than chlorine, on a per atom basis, to deplete ozone,[20] and that bromine reservoir compounds, compared to their chlorine analogues, have shorter lifetimes.[12,13,20,21] Although HBr chemistry *per se* involving eq 1 has been invoked by some authors,[22] the majority view[23] is instead that the relevant heterogeneous bromine chemistry involves the hydrolysis of bromine nitrate, $BrONO_2 + H_2O \rightarrow HOBr + HNO_3$, followed by reaction with HCl rather than HBr. In a similar vein, in nonpolar high latitudes, heterogeneous bromine chemistry is likely to involve the mixed reaction $HOBr + HCl \rightarrow BrCl + H_2O$ rather than HBr.[22,24,25]

In the mid-latitude stratosphere, away from the polar regions, where the relevant heterogeneous reaction media are highly acidic sulfate aerosols, the limited solubility of any halogen acid HX precludes their significant involvement, and again the relevant heterogeneous bromine chemistry involves $BrONO_2$ rather than HBr.[26]

The overall situation is evidently generally similar in the upper troposphere, where cirrus clouds are dominant: the higher concentration of HCl, compared to HBr, is thought to strongly favor the importance of chlorine-based heterogeneous chemistry.[27]

Evidently, by far, the most important role for HBr acid ionization occurs in the springtime Arctic tropospheric boundary layer, where bromine is much more abundant than elsewhere, and where heterogeneous bromine chemistry is implicated in extremely rapid ozone depletion near ground level.[28−30] Briefly, ozone-destroying Br radicals can be rapidly converted to the reservoir species HBr via gas-phase reactions involving formaldehyde and perhydroxyl.[31] In view of this, the heterogeneous reactions involving the reservoir species HBr

$$HBr + HOCl \rightarrow BrCl + H_2O \qquad (2)$$

$$HBr + HOBr \rightarrow Br_2 + H_2O \qquad (3)$$

are believed to be crucial in maintaining the readily photolyzable bromine species BrCl and Br_2, effective in gas-phase catalytic ozone destruction.[24,28,29,32] The relevant surfaces here include

† Part of the special issue "G. Wilse Robinson Festschrift".

* Corresponding author. E-mail: hynes@spot.colorado.edu, hynes@junie.ens.fr.

‡ Leiden University.

§ University of Colorado.

|| Ecole Normale Supérieure.

10.1021/jp020384a CCC: $22.00
Published on Web 06/18/2002

ice aerosols, snowpack ice, and sulfuric acid aerosols. HBr acid ionization would indicate ionic pathways involving the Br^- ion for the key reactions 2 and 3.

Experimental investigation of the interaction of HBr with ice was initiated by Hanson and Ravishankara,[9] who found unlimited uptake of HBr, in contrast to the limited uptake of HCl, under their experimental conditions. These authors pointed to the likelihood of acid ionization in this connection, noting the greater solution-phase acid strength of HBr compared to HCl, an inference reinforced by the experimentally observed feeble uptake of the weaker acid HF.[9] Indeed, we believe that this acid strength perspective is an extremely valuable one, and we will return to it.

The more facile uptake of HBr compared to HCl has been generally supported in subsequent experiments,[10,12−15] many of which have explored the formation of various hydrates of HBr under various experimental conditions. It appears, however, that under the low HBr pressure conditions that are atmospherically relevant, hydrate formation is unlikely.[13,14] In this case, the viability of the proton transfer eq 1 becomes the central issue for HBr, and we focus on it.

A number of more recent spectroscopic experimental results point to HBr ionization. Fourier transform infrared spectroscopy experiments[14] on thin ice films exposed to HBr at temperatures (e.g., 140 K) considerably lower than those relevant in the Arctic boundary layer (∼230−250 K[33]) suggest that HBr dissociates to form H_3O^+ and Br^- ions. Just as it has been pointed out for the case with HCl,[4] where low-temperature infrared observation of H_3O^+ [34] is complicated by the existence of hydrates, hydrate formation at low temperature may obscure the HBr ionization issue in the higher temperature atmospherically relevant context. It is also suggested[15] that the number of water molecules required for dissociation of HBr is smaller than that required for HCl. It is noteworthy that this would be in striking contrast to what would be expected on the basis of small cluster calculations, discussed below, where four water molecules are required for both HBr and HCl[16,17,35] (at 0 K).

On the theoretical side, there has been very limited activity for HBr reactivity on ice for related systems. An examination of HBr (and HCl) acid ionization on ice due to Robertson and Clary[18] utilized the quantum proton tunneling formulation of Borgis and Hynes[36] to conclude that acid ionization atop an ice surface was thermodynamically favorable for HBr (and HCl). However, as was pointed out already in ref 4, those calculations have certain difficulties, such that the conclusion does not follow.

Ionic dissociation has been investigated in very small $HBr\cdot(H_2O)_{1-4}$ water clusters via quantum chemical calculations.[16,17] The dissociated products Br^- and H_3O^+ are observed to be stable compared to undissociated HBr when the cluster contains four waters. In contrast to a simple contact ion pair, this observed ion pair has an unusual structure: a cycle of three water molecules separates the Br^- and H_3O^+ ions, each triply hydrogen-bonded above and below, respectively, the plane defined by the oxygens in the water cycle, in a trigonal-bipyramidal geometry (cf. ref 16). This persists as the most stable structure among all possibilities for the $HBr\cdot(H_2O)_4$ system up to about 180 K[16] (whereas the corresponding stability for a similar $Cl^-\cdot(H_2O)_3\cdot H_3O^+$ ion pair[35] has a more restricted temperature range). But in any event, it is important to emphasize that it is unclear exactly what degree of relevance such very small cluster studies have for the problem of acid dissociation on ice; in small clusters, the water molecules are free to extensively rearrange, in ways that might not be possible for an ice surface. As we will see, this is a relevant issue for much larger cluster models representative of an ice surface.

In this paper, we present quantum chemical calculations of larger cluster systems, $HBr\cdot(H_2O)_n(H_2O)_{13}$, $n = 0, 1$, as a model of HBr on ice. These calculations address the HBr ionization issue from a particular perspective. The $n = 0$ calculation explores the possibility that dissociation might occur atop a "dry" ice surface, an occurrence suggested not to be important for the weaker acid HCl.[37] The $n = 1$ calculation examines a situation where HBr dissociation might occur spontaneously with an additional extra-lattice water, a view consistent with a dynamic ice surface.[3,4,38]

Our computational results for a "dry" surface ($n = 0$) portray an endothermic HBr ionization. Conversely, we find that hydrogen bonding of the incipient Br^- anion by an extra-lattice water molecule ($n = 1$) results into the quite facile formation of a $H_30^+\cdot Br^-$ contact ion pair.

The outline of the remainder of this paper is as follows. In section 2, we describe and motivate the cluster model selected for the investigation. The HBr reaction on a "dry" ice surface via the $HBr\cdot(H_2O)_{13}$ cluster is described in section 3, whereas section 4 deals with the $HBr\cdot H_2O\cdot(H_2O)_{13}$ system. Concluding remarks are offered in section 5, including some comments on the comparison HCl case.

2. Choice of the Model System

The quantum chemical modeling of the interaction of HBr with an ice surface must take into account the natural structural constraints of the ice controlling the ability of lattice waters to hydrogen-bond to HBr or its derived $H_3O^+\cdot Br^-$ contact ion pair. Although a model ice lattice large enough to naturally enforce these constraints, at least locally, would obviously be desirable, its implementation from an ab initio perspective is not computationally viable. Therefore, guided by chemical intuition, one must resort to a computationally tractable model system where the perceived natural constraints are artificially enforced via an *ad hoc* selection of the internal coordinates (and their combinations) used to describe the dissociation process.

We choose as a model lattice a small section of the top bilayer of hexagonal ice, comprising thirteen water molecules arranged in three contiguous hydrogen-bonded rings, shown in Figure 1. This lattice model and the initial configuration used in the calculations are based on several considerations, such that the top bilayer is not exactly that of ideal hexagonal ice.[39] In particular, the structure of the ice portion studied here was taken from a molecular dynamics study ($T = 190$ K) of the sticking of molecular HCl on ice,[40] in which the ice surface was modeled by four dynamic bilayers superimposed on two bilayers of fixed water molecules. (This same HCl−ice configuration was found in ref 41.) In this way, the present modeling incorporates to a degree the influence of bilayers below the water molecules explicitly included. The water molecules in the first (top) monolayer are of two classes.[4,6,40] Each class contains three possible orientations of the hydrogen atoms of the water molecules. A class 1 water has one of its protons pointing perpendicular and away from the surface (exhibiting a "dangling bond"), while the second proton is pointing diagonally downward toward the bulk, forming a hydrogen bond with an oxygen of a water molecule in the second monolayer. A class 2 water has its two protons pointing downward toward the bulk, forming two hydrogen bonds with the neighboring waters in the second monolayer, and an electron lone pair pointing perpendicularly away from the surface.

The central water in the top monolayer of the model lattice in Figure 1 is of class 2 and is hydrogen-bonded to the HBr

proton, in a configuration close to that found in the study of ref 40 for HCl on ice (as will be seen in section 3.1, where geometric details are specified, this configuration is not far from the final optimized HBr configuration). This same water is also coordinated to three other waters in the second monolayer, offering considerable solvation in the eventuality of the formation of an H_3O^+ ion via proton transfer from HBr.[42]

In all our calculations, the general structure of the model lattice is preserved throughout the proton-transfer reaction by letting the nearest neighbor O−O distance (all initially set at the same value) in the oxygen atoms' framework vary simultaneously, while all the O−O−O angles and the O−O−O−O dihedral angles are kept fixed; this "breathing" motion of the lattice framework preserves the symmetry of the O-framework without, however, fixing the O atoms' positions. At the same time, all the OH bonds are independently allowed to vary, as are any angles involving H atoms; this improves the ability of the lattice to hydrogen-bond to HBr by letting all the OH bonds polarize and reorient.

The three internal coordinates best suited to examine the dissociation of HBr on top of an ice surface are (i) R, the distance between the H atom of HBr and the O atom of the proton-accepting central water molecule; (ii) r, the H−Br distance in HBr, and (iii) θ, the angle between the vectors **R** and **r**, and we use these in our discussions.

We used the quantum chemistry package GAMESS US.[43] All the calculations were carried out at the MP2[44] level using the −31-compatible SBKJC valence-only basis set (and its corresponding effective core potentials) for all the heavy atoms.[45] All the O atom basis sets are complemented with a polarization function (exp. 0.8), whereas the Br atom bears both polarization (exp. 0.389) and diffuse (exp. 0.0376) functions. In addition, the basis sets of the oxygens in the HBr-bound lattice central water and its three nearest neighbor waters (the latter meant to solvate the ensuing hydronium ion) is complemented with diffuse functions (exp. 0.0845). This selective assignment of basis functions for the $HBr{\cdot}(H_2O)_4$ core unit eases the computational burden by limiting the size of the basis set on lattice waters that have a merely solvating function (as opposed to electronic participation in the possible HBr dissociation), besides being consistent with recommendations in ref 46 for MP2 calculations on hydrogen-bonded systems.[47] Detailed structural data on the species examined are appended in the Supporting Information.

3. HBr Atop a Model $(H_2O)_{13}$ Ice Lattice

3.1. Reactant Complex. We first investigate the possible acid dissociation of HBr atop an ice lattice by optimizing the structure of the $HBr{\cdot}(H_2O)_{13}$ reactant complex shown in Figure 1. HBr is initially hydrogen-bonded to the accepting water at the center of the lattice, with an orientation almost perpendicular to the plane of the top monolayer. Specifically, via a series of preliminary optimizations at the Hartree−Fock level with smaller basis sets, we have selected the initial values of the reaction pair coordinates as follows: O−HBr distance R_o = 1.672 Å, H−Br distance R_o = 1.495 Å and the angle between r_o and R_o, $\theta_o = 168.4°$. The initial value of θ_o is similar to that found by Kroes and Clary[40] in their molecular dynamics study of the sticking of molecular HCl on ice. Throughout the geometry optimization, the ice lattice is semiconstrained, as described in section 2.[48]

We have found that HBr does not dissociate in this model system: molecular HBr is the stable species. In the optimized reactant complex, displayed in Figure 1, the H−Br bond length

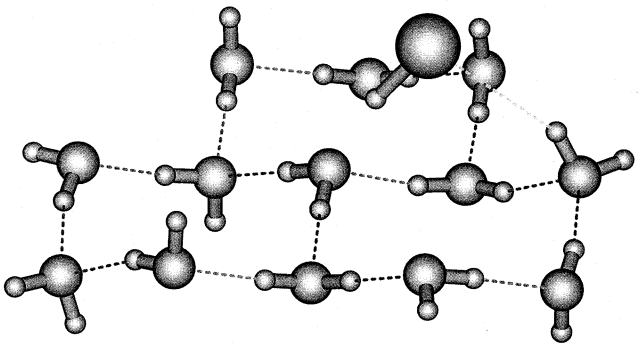

Figure 1. Optimized structure of HBr adsorbed on the basal plane face of a model hexagonal ice lattice comprising thirteen water molecules (R = 1.717 Å, r = 1.487 Å, and $\theta = 169.3°$). See section 3.1 for details.

r is 1.487 Å, whereas the O−HBr distance R is 1.717 Å, and $\theta_o = 169.3°$ (cf. Table A, Supporting Information).

It is apparent that HBr dissociation atop the model ice lattice is opposed by some significant barrier counter to the spontaneous formation of a $H_30^+{\cdot}Br^-{\cdot}(H_2O)_{12}$ contact ion pair via proton transfer. Such a barrier can be probed by forcing the model system to explore the region of the potential energy surface involving the proton transfer, via implementation of a strategy already used by two of us in studies of the mechanisms of the reactions of $ClONO_2$ with H_2O and HCl on ice.[7,37,49] We present these calculations in section 3.3.

3.2. Adsorption Energy of HBr on Ice. We have estimated the adsorption energy of HBr on the $(H_2O)_{13}$ model ice lattice corrected for basis set superposition error (BSSE)[50] according to the scheme $HBr^{(g)} + (H_2O)_{13}{}^{(g)} \rightarrow HBr^{(g)}{\cdot}(H_2O)_{(13)}{}^{(g)} \rightarrow HBr{\cdot}(H_2O)_{13}$, where the exponent "(g)" labels the monomers separately optimized, whereas the $HBr{\cdot}(H_2O)_{13}$ complex is the one optimized in the previous section.

The calculation has involved the following steps: (i) separate optimization of $HBr^{(g)}$ and $(H_2O)_{13}{}^{(g)}$ (the model lattice was optimized with the constraints described in section 3.1 above); (ii) optimization of the $HBr^{(g)}{\cdot}(H_2O)_{13}{}^{(g)}$ complex with both $HBr^{(g)}$ and $(H_2O)_{13}{}^{(g)}$ frozen into the optimized geometries obtained in the previous step (only the six intermolecular internal coordinates are relaxed); (iii) counterpoise (CP) correction[51] of the energy of $HBr^{(g)}$ and $(H_2O)_{13}{}^{(g)}$ in the presence of the entire basis set of the $HBr^{(g)}{\cdot}(H_2O)_{13}{}^{(g)}$ complex in the optimized geometry obtained in (ii); (iv) optimization of the $HBr{\cdot}(H_2O)_{13}$ complex via relaxation of the gas-phase optimized geometries of the monomers (performed in section 3.1 above). This scheme only corrects for the BSSE involved in the initial formation of the complex, without infringing upon the "natural" sharing of the dimer's whole basis set by the monomers to relax to their optimized geometries within the dimer. We find an adsorption energy corrected for BSSE of ∼9 kcal/mol (see Table 2).

3.3. Driven Heterolytic Dissociation of HBr in the Reactant Complex. To explore the energy penalty opposing acid dissociation, we have driven the optimized $HBr{\cdot}(H_2O)_{13}$ reactant complex along a dissociation path by constraining the O−HBr distance R at progressively smaller values in a stepwise fashion, and optimizing all remaining coordinates (still within the degrees of freedom of the semiconstrained lattice described in section 2). This compression procedure results in the heterolytic cleavage of the HBr bond and the production of a $H_3O^+{\cdot}Br^-$ contact ion pair. Relevant parameters are reported in Table 1.

The reported R values span the range in which one would expect a proton transfer barrier to appear. The driven dissociation yields a monotonic, increasing energy profile for R decreasing

TABLE 1: Driven Heterolytic Dissociation of HBr in $HBr\cdot(H_2O)_{13}$

R^a	r	θ	E(0 K)	ΔE^b	$q(H_3O^+)$	$q(Br^-)$
1.717[c]	1.487	169.3	−235.361502	0.00	0.31/0.37	−0.38/−0.36
1.50	1.535	169.4	−235.360586	0.57	0.36/0.40	−0.43/−0.42
1.40	1.574	169.1	−235.359550	1.22	0.40/0.42	−0.47/−0.44
1.30	1.632	168.6	−235.358250	2.04	0.45/0.45	−0.53/−0.48
1.20	1.720	166.7	−235.356801	2.95	0.51/0.52	−0.59/−0.52
1.10	1.889	161.5	−235.356154	3.36	0.60/0.66	−0.65/−0.57
1.05	1.969	160.0	−235.355932	3.50	0.64/0.69	−0.67/−0.60

[a] R and r in ångstroms, θ in degrees (see text for definitions), E(0 K) in hartree, ΔE in kcal/mol, Löwdin/Mulliken atomic charges $q(H_3O^+)$ and $q(Br^-)$ in e. [b] Energy relative to the E(0 K) energy of the optimized reactant complex. [c] First row: values corresponding to the optimized reactant complex.

TABLE 2: Energetics of the Adsorption of HBr on $(H_2O)_{13}$

	E(0 K)[a]	ΔE^b
$HBr^{(g)}$ [c]	−13.844564	
$(H_2O)_{13}{}^{(g)}$	−221.496506	
$HBr^{(g)} + (H_2O)_{13}{}^{(g)}$	−235.341070	12.8
$HBr^{(g)}\cdot(H_2O)_{13}{}^{(g)*}$ [d]	−13.847128	
$HBr^{(g)*}\cdot(H_2O)_{13}{}^{(g)}$	−221.499716	
$HBr + (H_2O)_{13}$ (CP corrected)	−235.346844	9.2
$HBr\cdot(H_2O)_{13}$	−235.361502	

[a] Absolute energy E(0 K) in hartree. [b] $\Delta E = E[HBr\cdot(H_2O)_{13}] - E[HBr + (H_2O)_{13}]$ in kcal/mol (1 hartree = 627.51 kcal/mol). [c] The exponent (g) labels the monomer geometries separately optimized.[d] The exponent * labels the "ghost" nuclei in the CP correction calculation.

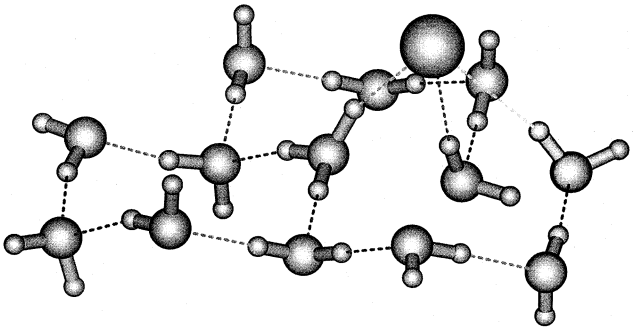

Figure 2. Structure of the $Br^-\cdot(H_3O)^+\cdot(H_2O)_{12}$ contact ion pair (R = 1.05 Å, r = 1.969 Å, and θ = 160.0°) obtained via driven dissociation of HBr in the reactant complex shown in Figure 1. See section 3.3 for details.

from 1.717 to 1.05 Å, the latter value representative of the OH bond length in hydronium ion in this model environment (see Appendix A). The H_3O^+ and Br^- charges reported in Table 1 are indicative of the transition from molecular pair to contact ion pair, and resemble, for R = 1.05 Å those of independently solvated H_3O^+ and Br^- (see Appendix A).

The structure of the contact ion pair for R = 1.05 Å is displayed in Figure 2. The OH bonds in the central H_3O^+ are 1.05 (pointing toward Br), 1.04 (pointing toward the observer), and 1.01 Å, respectively, whereas the HOH angles are 112°, 112°, and 120° (the last between the OH bond pointing away from the observer and the one pointing toward Br). The bromide ion is solvated by three hydrogen bonds: one with H_3O^+ (1.969 Å), and the others with two lattice waters (2.417 and 2.550 Å, the latter with the rightmost water). We note that one of these two waters was initially hydrogen-bonded to the central water (now H_3O^+). The formation of the hydronium ion has weakened the original hydrogen bond and allowed the formation of a hydrogen bond to the bromide ion, leaving the hydronium ion tricoordinated, a local arrangement previously discussed in ref 52.

Although the energy values in Table 1 are calculated at 0 K, their trend strongly indicates that the formation of the contact ion pair is endothermic for the $HBr\cdot(H_2O)_{13}$ model system. We could not calculate the zero point energy (ZPE) contribution to the driven dissociation minimum energy path, since the presence of lattice constraints yields several imaginary frequencies in the diagonalization of the Hessian matrix along the constrained path. However, the ZPE correction for the related case of acid dissociation of HCl on ice is in favor of the contact ion pair, and can account for at most 2 kcal/mol stabilization relative to the neutral pair.[4] Thus, even assuming a barrier decrease of 2 kcal/mol due to ZPE correction, the driven dissociation path for $HBr\cdot(H_2O)_{13}$ remains endothermic.

This conclusion is not affected by the absence of further waters in our model lattice. In fact, extra water layers attached "underneath" the three-rings model lattice could only reduce the ability of the OH bonds to reorient and solvate the Br^- ion. Thus, given the bias *in favor* of HBr dissociation, the endothermicity observed for the driven formation of $H_3O^+\cdot Br^-$ without any extra water present (cf. Figure 2) is a *lower* estimate, since extra waters would certainly impede the rotation of the OH initially bound to the central water lone pair, and the consequent lack of solvation for Br^- would lead to an energy for the contact ion pair *higher* than the one currently reported in Table 1. Similar remarks also apply to the rightmost, edge water in Figure 2.

As an important concluding remark in this section, we note that these studies of the "dry" $HBr\cdot(H_2O)_{13}$ case highlight the role of lattice constraints in opposing acid dissociation: their presence prevents the collapse of the cluster during geometry optimization, an event conducive to structures representative of gas-phase clusters known to promote dissociation,[16] but extraneous to the present context.

4. The $HBr\cdot H_2O$ Complex Atop a Model $(H_2O)_{13}$ Ice Lattice

The "dry" $HBr\cdot(H_2O)_{13}$ model system studied in section 3 neglects the participation of further waters, extra-lattice, which could assist in the dissociation. This general feature was invoked by Gertner and Hynes[3,4] in connection with HCl acid dissociation under polar stratospheric conditions (~190 K), in view of the dynamic character of the ice surface under those conditions.[38,53] This aspect should be even more important at the higher temperature and humidity conditions in the Arctic tropospheric boundary layer.[33]

In this section, we probe the ability of HBr to ionize in the presence of one extra water molecule, adsorbed on the lattice and hydrogen-bonded to bromine. This scenario, in which HBr is in a ring of water molecules, was viewed in the comparison HCl case[3,4] as leading to HCl incorporation *at* the ice surface, followed by dissociation. The question addressed in this section for HBr is if this stronger acid can dissociate even at this stage, without complete incorporation into the lattice.

The $HBr\cdot H_2O\cdot(H_2O)_{13}$ model system chosen for the calculations is displayed in Figure 3. The initial O−HBr distance, R_o = 1.672 Å, and H−Br distance, r_o = 1.495 Å, are those also chosen for the initial configuration of the $HBr\cdot(H_2O)_{13}$ reactant complex in section 3.1, with the extra water grafted on to the lattice in a reasonable location. Again, the O-framework bears the only structural constraints, similar to previous sections, while both HBr and the extra water are unconstrained.

The geometry optimization of the $HBr\cdot H_2O\cdot(H_2O)_{13}$ complex leads to heterolytic dissociation of HBr with formation of a $H_3O^+\cdot Br^-\cdot(H_2O)_{13}$ contact ion pair, shown in Figure 4. The

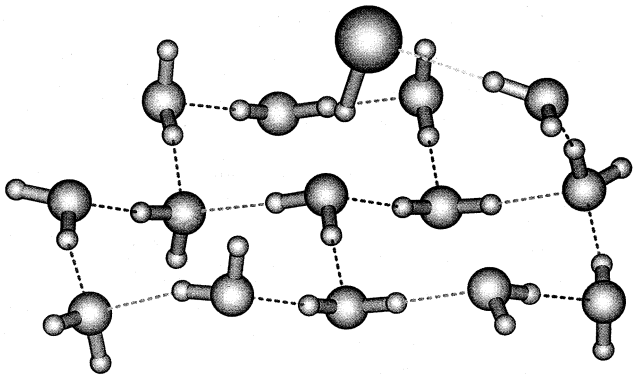

Figure 3. Initial configuration of $HBr \cdot H_2O$ adsorbed on the $(H_2O)_{13}$ model ice lattice. See section 4 for details.

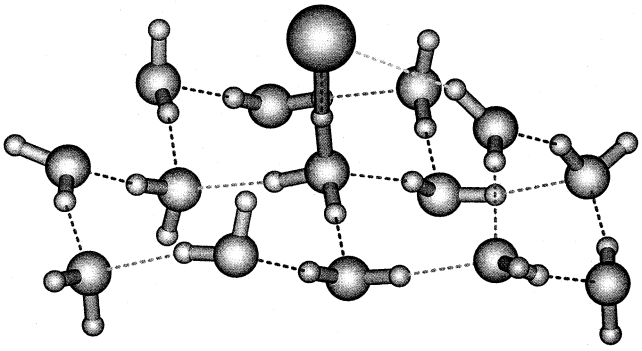

Figure 4. Structure of the $Br^- \cdot (H_3O)^+ \cdot (H_2O)_{13}$ contact ion pair derived from the $HBr \cdot H_2O \cdot (H_2O)_{13}$ complex displayed in Figure 3 via simple geometry optimization ($R = 1.17$ Å, $r = 1.773$ Å, and $\theta = 173.2°$). See section 4 for details.

presence of H_3O^+ in the stable structure is signaled by the strongly reduced O−HBr distance R to a value of 1.166 Å, indicative of a polarized OH bond in the hydronium ion (see Appendix A). This view is also supported by the final lengths of the other two OH bonds in the proton-accepting water, increased to 1.035 (pointing toward the observer) and 1.017 Å from, respectively, 1.011 and 1.000 Å in the starting structure. The HOH angles in this hydronium ion are 107°, 102°, and 103°. The H−Br distance r has increased to 1.773 from 1.672 Å. The OHBr angle is 173°. The extra water, forming a hydrogen bond of 2.501 Å with Br^-, is also hydrogen-bonded to two other waters of the lattice.

The Löwdin/Mulliken atomic charges on H_3O^+ and Br^- are 0.53/0.50 and −0.63/−0.55 e, respectively (cf. Appendix A). Similar to the driven dissociation case of Figure 2, although in a much less pronounced fashion, the hydrogen bond between the electron lone pair of the ensuing H_3O^+ and the lattice water in the second monolayer has noticeably weakened,[4,52] as signaled by the changed orientation of the water OH bond relative to Figure 3, thus providing further support to the cationic nature of the central H_3O moiety.

Solvation for the incipient Br^- ion is provided mostly by the extra-lattice water, requiring a far milder reorientation of the OH bond oriented toward the (weak) lone pair of the central, incipient H_3O^+ (compare Figures 2 and 4). This is clearly a case where the presence of further water layers underneath would presumably have little influence on the observed barrierless HBr dissociation.

5. Concluding Remarks

We have found that the HBr heterolytic dissociation on top of a semiconstrained model ice surface is endothermic by an estimated 3.5 kcal/mol (without ZPE correction). However, when an extra water molecule is added to the model system, adsorbed on the ice lattice and hydrogen-bonded to bromine, HBr is found to dissociate spontaneously to form a $H_3O^+ \cdot Br^-$ contact ion pair, with the hydronium ion solvated by the waters in the top bilayer and the bromide ion, the latter also solvated by the extra water.[54] The ion pair structure is not the one found in small cluster calculations,[16,17] emphasizing the importance of constraints imposed by an ice lattice.

The implications of these results for the Arctic boundary layer reactions of HBr with HOCl and HOBr (eqs 2 and 3) is that, clearly, they will occur via ionic mechanisms. The reaction of Cl^- with HOCl has already been considered theoretically,[55] although the issue of any role of H_3O^+ in that reaction[49] (as for the reaction of HCl with $ClONO_2$[7]) remains to be examined.

The present HBr results call for a comparison with HCl. In related calculations,[56] we have found that the corresponding acid ionization for HCl does not occur until two extra water molecules are present atop the model ice lattice. These HCl results will be placed in perspective with assorted literature results connected with mechanisms of HCl ionization involving HCl incorporation at a dynamic ice surface or ionization atop a "dry" ice surface[3,4,8,37,41,57] in an extensive discussion elsewhere.[56] Here we restrict our discussion to why HBr would require fewer waters than HCl to dissociate atop the ice. As stressed in refs 3, 4, and 37, a crucial aspect is the necessary solvation of an incipient Cl^- ion, essential for a favored dissociation[52] (over and above the solvation requirements for an incipient H_3O^+). From this perspective, the more facile dissociation of HBr atop the surface would have to be driven by the *increased acid strength* of HBr compared to that of HCl. In the current understanding of hydrohalic acid HX relative acid strength in solution,[52,58] the ordering HF < HCl < HBr < HI traces to the decreasing homolytic H−X bond strength in the series. Since this ordering is opposite of the anion solvation free energies in water,[59] e.g., Br^- is less well solvated than Cl^-, the solvation of Br^- is *less* important for HBr dissociation than the solvation of Cl^- is for HCl dissociation; only one extra water is required for HBr while HCl requires two. In this connection, we also note that if the surface of ice doped with HCl were well described as a "liquid-like layer",[60] which is not observed in assorted simulations at ∼190 K,[3,4,8] there would presumably be no distinction between the ease of acid dissociation of HBr and HCl, due to the leveling effect of strong acids.[58]

Acknowledgment. This work was supported in part by the NSF grants ATM-9613802, ATM-0000542, and CHE-9709195 and the CNRS. This work is part of the program of FOM that is financially supported by NWO. A.Al-H. thanks Drs. J. E. van Dierendonck for financial support and G. J. Kroes for a careful reading of the manuscript. J.T.H. thanks Prof. M. Tolbert for useful discussions.

A. Reference Structural Parameters for the $H_3O^+ \cdot (H_2O)_3$ and $Br^- \cdot (H_2O)_3$ Ions

To identify reference features of solvated H_3O^+ and Br^- ions within the level of theory used, we have optimized the geometry of the $H_3O^+ \cdot (H_2O)_3$ and $Br^- \cdot (H_2O)_3$ model clusters, with H_3O^+ and Br^- at the center of the clusters, hydrogen-bonded to the surrounding waters. In both cases, to simulate the surface environment, structural constraints have been enforced during the optimization. In particular, the distances between the central heavy atom (O/Br) and the oxygens of the solvating waters have been fixed at 2.81 Å, whereas all the OXO (X = O, Br) angles

have been kept near-tetrahedral (109.71°). In the $H_3O^+ \cdot (H_2O)_3$ case, no other constraints were imposed, whereas for the $Br^- \cdot (H_2O)_3$ case, the hydrogen bonds were kept collinear. In both cases, the OH bonds were unconstrained.

For H_3O^+ in the optimized $H_3O^+ \cdot (H_2O)_3$ cluster, the OH distance averages 1.031 Å, whereas the HOH angles are 108.6°. The Löwdin/Mulliken atomic charges of H_3O^+ and Br^- in their respective complexes are 0.84/0.93 and −0.48/−0.59 *e*, respectively.

Supporting Information Available: Structures and energies of the following clusters: optimized $HBr \cdot (H_2O)_{13}$ reactant complex; forcibly dissociated $Br^- \cdot (H_3O)^+ \cdot (H_2O)_{12}$; $HBr \cdot H_2O \cdot (H_2O)_{13}$ in its initial configuration; optimized $Br^- \cdot (H_3O)^+ \cdot (H_2O)_{13}$ contact ion pair; optimized $H_3O^+ \cdot (H_2O)_3$; optimized $Br^- \cdot (H_2O)_3$. This material is available free of charge via the Internet at http://pubs.acs.org.

References and Notes

(1) Solomon, S.; Garcia, R. R.; Rowland, F. S.; Wuebbles, D. J. *Nature* **1986**, *321*, 755.

(2) Solomon, S. *Rev. Geophys.* **1999**, *37*, 275. Seinfield, J. H.; Pandis, S. N. *Atmospheric Chemistry and Physics. From Air Pollution to Climate Change*; Wiley-Interscience: New York, 1998. Kolb, C. E.; Worsnop, D. R.; Zahniser, M. S.; Davidovits, P.; Keyser, L. F.; Leu, M.-T.; Molina, M. J. Hanson, D. R.; Ravishankara, A. R.; Williams, L. R.; Tolbert, M. A. Laboratory Studies of Atmospheric Heterogeneous Chemistry. In *Progress and Problems in Atmospheric Chemistry*; Barker, J. R., Ed.; World Scientific Publishing Co.: NJ, 1995. Peter, T. *Annu. Rev. Phys. Chem.* **1997**, *48*, 785. Molina, M. J.; Molina, L. T.; Kolb, C. E. *Annu. Rev. Phys. Chem.* **1996**, *47*, 327. Abbatt, J. P. D.; Molina, M. J. *Annu. Rev. Energy Environ.* **1993**, *18*, 1. Toohey, D. W. *Rev. Geophys.* **1995**, *33*, 759, Part 2, Suppl. S.

(3) Gertner, B. J.; Hynes, J. T. *Science* **1996**, *271*, 1563.

(4) Gertner, B. J.; Hynes, J. T. *Faraday Discuss.* **1998**, *110*, 301.

(5) Clary, D. C.; Wang, L. C. *J. Chem. Soc., Faraday Trans.* **1997**, *93*, 2763.

(6) Kroes, G. J. *Adv. At. Mol. Phys.* **1999**, *34*, 259.

(7) Bianco, R.; Hynes, J. T. *J. Phys. Chem. A* **1999**, *103*, 3797.

(8) Svanberg, M.; Pettersson, J. B. C.; Bolton, K. *J. Phys. Chem. A* **2000**, *104*, 5787. Bolton, K.; Petterson, J. B. C. *J. Am. Chem. Soc.* **2001**, *123*, 7360.

(9) Hanson, D. R.; Ravishankara, A. R. *J. Phys. Chem.* **1992**, *96*, 9441.

(10) Abbatt, J. P. D. *Geophys. Res. Lett.* **1994**, *21*, 665. Chu, L. T.; Heron, J. W. *Geophys. Res. Lett.* **1995**, *22*, 3211. Delzeit, L.; Rowland, B.; Devlin, J. P. *J. Phys. Chem.* **1993**, *97*, 10312. Gilbert, A. S.; Sheppard, N. *J. Chem. Soc., Faraday Trans. 2* **1973**, *69*, 1628. Lundgren, J.-O. *Acta Crystallogr.* **1970**, *B26*, 1893. Gilligan, J. J.; Castleman, A. W. *J. Phys. Chem. A* **2001**, *105*, 5601. Fluckiger, B.; Chaix, L.; Rossi, M. J. *J. Phys. Chem. A* **2000**, *104*, 11739. Carlo, S. R.; Grassian, V. H *J. Phys. Chem. B* **2000**, *104*, 86. Fluckiger, B.; Thielmann, A.; Gutzwiller, L.; Rossi, M. J. *Ber. Bunsen-Ges. Phys. Chem.* **1998**, *102*, 915.

(11) Percival, C. J.; Mössinger, J. C.; Cox, R. A. *Phys. Chem. Chem. Phys.* **1999**, *1*, 4565.

(12) Rieley, H.; Aslin, H. D.; Haq, S. *J. Chem. Soc., Faraday Trans.* **1995**, *91*, 2349.

(13) Chu, L. T.; Chu, L. *J. Phys. Chem. A* **1999**, *103*, 384.

(14) Hudson, P. K.; Foster, K. L.; Tolbert, M. A.; George, S. M.; Carlo, S. R.; Grassian, V. H. *J. Phys. Chem. A* **2001**, *105*, 694.

(15) Barone, S. B.; Zondlo, M. A.; Tolbert, M. A. *J. Phys. Chem. A* **1999**, *103*, 9717.

(16) Gertner, B. J.; Peslherbe, G. H.; Hynes, J. T. *Isr. J. Chem.* **1999**, *39*, 273.

(17) Conley, C.; Tao, F. M. *Chem. Phys. Lett.* **1999**, *301*, 29.

(18) Robertson, S. H.; Clary, D. C. *Faraday Discuss.* **1995**, *100*, 309.

(19) Anderson, J. G.; Brune, W. H.; Lloyd, S. A.; Toohey, D. W.; Sander, S. P.; Starr, W. L.; Loewenstein, M.; Podolske, J. R. *J. Geophys. Res.—Atmos.* **1989**, *94*, 11480. McElroy, M. B.; Salawitch, R. J.; Wofsy, S. C.; Logan, J. A. *Nature* **1986**, *321*, 759. Solomon, S.; Sanders, R. W.; Miller, H. L. *J. Geophys. Res.—Atmos.* **1990**, *95*, 13807.

(20) *Scientific assessment of Ozone Depletion: 1994*; WMO: Geneva, Switzerland, 1995.

(21) Wayne, R. P. *Chemistry of Atmospheres*, 2nd ed.; Oxford University Press: Oxford, NY, 1991. Jobson, B. T.; Niki, H.; Yokouchi, Y.; Bottenheim, J.; Hopper, F.; Leaitch, R. *J. Geophys. Res.—Atmos.* **1995**, *100*, 25355.

(22) Lary, D. J.; Chipperfield, M. P.; Toumi, R.; Lenton, T. *J. Geophys. Res.—Atmos.* **1996**, *101*, 1489.

(23) Danilin, M. Y.; McConnell, J. C. *J. Geophys. Res.—Atmos.* **1994**, *99*, 25681; **1995**, *100*, 11237.

(24) Waschewsky, G. C. G.; Abbatt, J. P. D. *J. Phys. Chem. A* **1999**, *103*, 5312.

(25) Tie, X. X.; Brasseur, G. *Geophys. Res. Lett.* **1996**, *23*, 2505. Fish, D. J.; Aliwell, S. R.; Jones, R. L. *Geophys. Res. Lett.* **1997**, *24*, 1199. Abbatt, J. P. D. *J. Geophys. Res.—Atmos.* **1995**, *100*, 14009.

(26) Robinson, G. N.; Worsnop, D. R.; Jayne, J. T.; Kolb, C. E.; Davidovits, P. *J. Geophys. Res.—Atmos.* **1997**, *102*, 3583.

(27) Solomon, S.; Borrmann, S.; Garcia, R. R.; Portmann, R.; Thomason, L.; Poole, L. R.; Winker, D.; McCormick, M. P. *J. Geophys. Res.—Atmos.* **1997**, *102*, 21411. Borrmann, S.; Solomon, S.; Dye, J. E.; Luo, B. P. *Geophys. Res. Lett.* **1996**, *23*, 2133. Reichardt, J.; Ansmann, A.; Serwazi, M.; Weitkamp, C.; Michaelis, W. *Geophys. Res. Lett.* **1996**, *23*, 1929.

(28) Niki, H., Becker, K. H., Eds. *The Tropospheric Chemistry of Ozone in the Polar Regions*; NATO ASI Series; Series I, Global Environmental Change, Vol. 7; Springer-Verlag: New York, 1993.

(29) Fan, S. M.; Jacob, D. J. *Nature* **1992**, *359*, 522. Barrie, L. A.; Bottenheim, J. W.; Schnell, R. C.; Crutzen, P. J.; Rasmussen, R. A. *Nature* **1988**, *334*, 138. Barrie, L. A. *Features of Polar Regions Relevant to Tropospheric Ozone*; NATO ASI Series; Series I, Global Environmental Change, Vol. 7; Springer-Verlag: New York, 1993; pp 3−24.

(30) McConnell, J. C.; Henderson, G. S.; Barrie, L.; Bottenheim, J.; Niki, H.; Langford, C. H.; Templeton, E. M. J. *Nature* **1992**, *355*, 150.

(31) Sumner, A. L.; Shepson, P. B. *Nature* **1999**, *398*, 230. DeMore, W. B., et al., Eds. *Chemical Kinetics and Photochemical Data for Use in Nasa Jet Propulsion Laboratory*; JPL: Pasadena, CA, 1997.

(32) McConnell, J. C.; Henderson, G. S. *Features of Polar Regions Relevant to Tropospheric Ozone*; NATO ASI Series; Series I, Global Environmental Change, Vol. 7; Springer-Verlag: New York, 1993; pp 89−103. Abbatt, J. P. D.; Nowack, J. B. *J. Phys. Chem. A* **1997**, *101*, 2131.

(33) Leaitch, W. R.; Hoff, R. M.; MacPherson, J. T. *J. Atmos. Chem.* **1989**, *9*, 187.

(34) Horn, A. B.; Chesters, M. A.; McCoustra, M. R. S.; Sodeau, J. R. *J. Chem. Soc., Faraday Trans.* **1992**, *88*, 1077.

(35) Lee, C. T.; Sosa, M.; Planas, M.; Novoa, J. J. *J. Chem. Phys.* **1996**, *104*, 7081. Re, S.; Osamura, Y.; Suzuki, Y.; Schaefer, H. F. *J. Chem. Phys.* **1998**, *109*, 973.

(36) Borgis, D.; Hynes, J. T. *J. Chem. Phys.* **1991**, *94*, 3619.

(37) Bianco, R.; Gertner, B. J.; Hynes, J. T. *Ber. Bunsen-Ges. Phys. Chem.* **1998**, *102*, 518.

(38) Haynes, D. R.; Tro, N. J.; George, S. M. *J. Phys. Chem.* **1992**, *96*, 8502.

(39) See e.g.: Davidson, E. R.; Morokuma, K. *J. Chem. Phys.* **1984**, *81*, 3741.

(40) Kroes, G. J.; Clary, D. C. *J. Phys. Chem.* **1992**, *96*, 7079.

(41) Bussolin, G.; Casassa, S.; Pisani, C.; Ugliengo, P. *J. Chem. Phys.* **1998**, *108*, 9516.

(42) One might be concerned that electric field effects arising from omitted waters below our model lattice might be of significance. Arguments can however be presented that this is not the case. We can estimate the dipolar field at the central oxygen, hydrogen-bonded to HBr, due to a water in the first (top) monolayer of a hypothetical second bilayer underneath the current three-rings model lattice. For an ideal O−O distance of 2.75 Å and approximately tetrahedral OOO angles (∼110°), the shortest O−O distance between the central O and the closest water in the bilayer below is ∼4.5 Å. The ratio of the moduli of the electric field vectors $E_{near} \propto 1/r_{near}^3$ and $E_{far} \propto 1/r_{far}^3$ due to two pointlike electric dipoles of the same modulus at distances $r_{near} = 2.75$ Å and $r_{far} = 4.5$ Å from the same point is $(r_{near}/r_{far})^3 \simeq 0.23$. Thus the dipolar field due to one water in the second bilayer closest to the central oxygen in the top bilayer is only one-fifth of that due to a nearest neighbor water in the top bilayer. The lack of an explicit second bilayer underneath the three-rings model lattice is therefore an acceptable approximation.

(43) Schmidt, M. W.; Baldridge, K. K.; Boatz, J. A.; Elbert, S. T.; Gordon, M. S.; Jensen, J. H.; Koseki, S.; Matsunaga, N.; Nguyen, K. A.; Su, S. J.; Windus, T. L.; Dupuis, M.; Montgomery, J. A. *J. Comput. Chem.* **1993**, *14*, 1347.

(44) Möller, C.; Plesset, M. S. *Phys. Rev.* **1934**, *46*, 618.

(45) Stevens, W. J.; Krauss, M.; Basch, H.; Jasien, P. G. *Can. J. Chem.* **1992**, *70*, 612. Stevens, W. J.; Basch, H.; Krauss, M. *J. Chem. Phys.* **1984**, *81*, 6026.

(46) Del Bene, J. E.; Jordan, M. J. T. *Int. Rev. Phys. Chem.* **1999**, *18*, 119.

(47) All results presented in the present work were obtained with the default integral accuracy provided by the INTTYP=POPLE option in GAMESS. Subsequent recalculation of energies and gradients for local minima and the driven ionization path in section 3.3 with the more accurate INTTYP+HONDO option, recommended for the use of diffuse functions at MP2 level, yielded energies only 10^{-6} hartree lower relative to those obtained with the INTTYP+POPLE option, and corresponding gradients below the 10^{-4} hartree/bohr acceptance threshold.

(48) The OO separation in the ice lattice for the optimized $HBr\cdot(H_2O)_{13}$ complex is 2.85 Å, slightly larger than the value 2.75 Å for hexagonal ice [Kuhs, W. F.; Lehmann, M. S. *J. Phys. Chem.* **1983**, *87*, 4312]. This magnitude of discrepancy is quite common for finite lattice models [Liu, K.; Brown, M. G.; Carter, C.; Saykally, R. J.; Gregory, J. K.; Clary, D. C. *Nature* **1999**, *381*, 501. Sadlej, J.; Buch, V.; Kazimirski, J. K.; Buck, U. *J. Phys. Chem. A* **1999**, *103*, 4933. Sadlej, J. *Chem. Phys. Lett.* **2001**, *333*, 485]. We do not consider this a serious discrepancy, but it would be of interest to examine more extended model lattice systems in the future.

(49) Bianco, R.; Hynes, J. T. *J. Phys. Chem. A* **1998**, *102*, 309.

(50) van Duijneveldt, F. B.; van Duijneveldt-van De Rijdt, J. G. C. M.; van Lenthe, J. H. *Chem. Rev.* **1994**, *94*, 1873.

(51) Boys, S. F.; Bernardi, F. *Mol. Phys.* **1970**, *19*, 553.

(52) Ando, K.; Hynes, J. T. *J. Mol. Liq.* **1995**, *64*, 25; *J. Phys. Chem. B* **1997**, *101*, 10464; *Faraday Discuss.* **1995**, *102*, 435.

(53) Andersson, P. U.; Någård, M. B.; Pettersson, J. B. C. *J. Phys. Chem. B* **2000**, *104*, 1596.

(54) Based on acid strength, we would expect a behavior for HI similar to that of HBr. Experimental data (Chu, L. T.; Chu, L. *J. Phys. Chem. B* **1997**, *101*, 6271 and refs 11 and 15) show an order of magnitude higher uptake of HI compared to HCl, but very much the same as the uptake of HBr.

(55) Liu, Z. F.; Siu, C. K.; Tse, J. S. *Chem. Phys. Lett.* **1999**, *311*, 93.

(56) Bianco, R.; Al-Halabi, A.; Hynes, J. T. Acid dissociation of HCI on a model ice surface, to be submitted.

(57) Mantz, Y. A.; Geiger, F. M.; Molina, L. T.; Molina, M. J.; Trout, B. L. *Chem. Phys. Lett.* **2001**, *348*, 285. Estrin, D. A.; Kohanoff, J.; Laria, D. H.; Weht, R. O. *Chem. Phys. Lett.* **1997**, *280*, 280. Allouche, A.; Couturier-Tamburelli, I.; Chiavassa, T. *J. Phys. Chem. B* **2000**, *104*, 1497. Casassa, S. *Chem. Phys. Lett.* **2000**, *321*, 1. Toubin, C.; Hoang, P. N. M.; Picaud, S.; Girardet, *C. Chem: Phys. Lett.* **2000**, *329*, 331.

(58) See, e.g.: Silberberg, S. *Chemistry: The molecular Nature of Matter and Change*, 2nd ed.; McGraw-Hill: New York, 2000; Chapter 18.

(59) Marcus, Y. *Ion Solvation*; Wiley: Chichester, U.K., 1985.

(60) See, e.g.: Abbatt, J. P. D.; Beyer, K. D.; Fucaloro, A. F.; McMahon, J. R.; Wooldridge, P. J.; Zhang, R.; Molina, M. J. *J. Geophys. Res.—Atmos.* **1992**, *97*, 15819 and references therein.